Supplemental Table 1. Primary antibodies[i].

antibodies:	*label*	*source*	*conc.*	*assays*	*immunogen*	*purification*	*specificity, comments*[ii]
gt anti-Lmα4	gt anti-Lmα4	R&D, AF3837	1 μg/ml	ELISA	LG peptide (res. Gln826-Ala1816)		ELISA: rLm411 – half-max binding = 0.3 μg/ml, Lm211 not detected at 10 μg/ml.
ch anti-ms Lmα4	ch anti-Lmα4	this study	1 μg/ml	ELISA, IF	rLm411 (ms α4)	XA: rLm211, Lm/Nd, rLm511+rNd; AP: rLm411	ELISA: rLm411 - half-max = 0.2 μg/ml, No rLm211 cross-reactivity detected >0 - 10 μg/ml. WB: reacts with Lmα4 but not other Lm subunits. IF: muscle vessels and peripheral nerve staining.
ch anti-ms Lmα5	anti-Lmα5	this study	1 μg/ml	ELISA, IF	rLm511 (ms α5)	XA: r2Lm11, EHS-Lm/Nd; AP: rLm511	ELISA: rLm511 half-max = 1 μg/ml. No rLm211 reactivity at 2 μg/ml, 15% at 10 μg/ml. WB: reacts with Lmα5 but not other Lm subunits. IF: muscle vessels immunostained.
rt anti-Lmγ1 (mAb)	rt anti-Lmγ1	Millipore, MAB1914P. (Chemicon)	1:100, 10μg/ml	IF	ms-Lm111		IF: Specific for BMs. Used to immunostain muscle.
ms anti-Lmγ1 (mAb)	ms anti-Lmγ1	Millipore, MAB1920	1:250 (ascites)	IF	ms-Lm111		IF: Specific for BMs. Used to immunostain C2C12.
rb anti-Lmα2–ΔLG1-5	anti-Lmα2–ΔLG	this study	1 μg/ml	ELISA	hu rLm211ΔLG1-5	XA: rLm411, Lm/Nd; AP: rLm211, rLmα2ΔLG1-5	ELISA: rLm211 – half-max=0.2 μg/ml. rLm111 – 15% binding at 2 μg/ml with no increase by 5 μg/ml. WB: reacts with Lmα2 but not other Lm subunits.
rt anti hu Lmα2 (mAb)	anti-Lmα2 (L4b)	Sigma, L-0663	2 μg/ml	IF			Allamand 1997: Lmα2-L4b domain specificity.
ch anti-hu Lmβ1γ1	ch anti-Lmβ1γ1	this study	1 μg/ml	ELISA	rLm511 (ms Lmα5)	AP: rLm211; XA: rNd	ELISA: At 1 μg/ml reacts with rLms but not Nd.; IB: reacts with Lmβ1γ1 chains of rLms.
rb anti-hu Lmα2LG1-5		Cheng 1997	1 μg/ml	WB	hu rLmα2-LG1-5		ELISA: rLm211, half-max=0.1 μg/ml. Does not react with rLm111 below 2 μg/ml; IB: 75 kDa Lmα2 LG band detected in WT but not dy3K muscle. IF: Stains WT muscle but not dy3K (Lmα2-knockout) muscle.
rb anti-Lm111 (minus α1LN-L4b short arm)	anti-Lm*	this study	1 μg/ml	ELISA, WB	EHS-Lm111	AP: EHS-Lm111, XA: rLm211, rNd, F2	ELISA: rLm211, half-max=0.5 μg/ml, rNd1, not detected at 40 μg/ml; F2 not detected at 40 μg/ml. Binds to fragment E4 (Lmβ1LN-LEa), rLm111, rLm121. WB: reacts with Lmβ1/γ1, faintly with Lmα1, and not with Lmα2, Lmα5.
rb anti-ms collagen-IV	anti-Col-IV	Millipore, AB765P	0.5 μg/ml	IF			IF: Muscle BM staining that is lost after treatment with bacterial collagenase.
ch anti rLmα1LN-L4bmANta	ch anti-F2 (used to detect/bind αLNNd)	this study	1 μg/ml	ELISA, WB	ms rLmα1LN-L4b-mANta chimeric fusion protein ("F2")	XA: rLm211,Nd; AP: F2	ELISA: rLm111 – half-max=0.2 μg/ml; rLm211– no binding at 1 μg/ml, 8% binding at 10 μg/ml; Nd1-not detected at 8 μg/ml, ~10% at 20 μg/ml. WB: reacts with Lmα1 and αLNNd but not Nd, Lmα2, α4, α5. IF: stains BM in αNNd transgenic muscle but not WT or dy2J muscle.
gt anti-hu Lmα1 N-terminus domain VI (LN)	gt anti-Lmα1LN	R&D Syst., AF4187	1 μg/ml	WB	E.coli Lmα1 peptide Leu22-Met269.	antigen-AP	Used for initial screens by WB.
rb anti ms Lmβ1	anti-Lmβ1	Li, 2002	1-5 μg/ml	ELISA	EHS Lm111, frag. E4		In WB, only reacts with non-reduced Lm111 and E4.
ms anti-αDG (IgM mAb IIH6)	anti-αDG	Millipore. 05-593,	1:100 ascites	IF			
rt anti-β1 integrin (mAb)	anti-Itg β1	Millipore mAb 1997	20 μg/ml	IF			
rb anti-ms nidogen-1	anti-Nd	Li, 2002	1 μg/ml	IF	ms rNidogen-1		
rb anti-ms nidogen-1 G2-G3	anti-NdG2-G3 (used to detect αLNNd and Nd1)	this study	1 μg/ml, IP 5μg/ml	ELISA, IP, WB	ms rNidogen-1	AP: αLNNd; XA: F2.	ELISA: rNd, half-max<0.05 μg/ml; rLm111 > 20 μg/ml.

[i] Abbreviations: (a) gt, goat; ch, chicken; rb, rabbit; ms, mouse; rt, rat; hu, human; WB, western blot; IP, immunoprecipitation; IF, immunofluorescence. (b) Lm, laminin; Nd, nidogen-1; Col-IV. collagen-IV; r, recombinant protein; αDG, α-dystroglycan, Itg, integrin; (c) AP, affinity purified on immobilized column; XA, cross-absorbed against gel-immobilized protein.

[ii] ELISA coat, rLm411 (1 μg/ml), rLm511 (1 μg/ml), rLm111 (1 μg/ml). WBs performed with rLm111, rLm211, rLm411, rLm511, αLNNd, rNd-1 (reducing conditions).

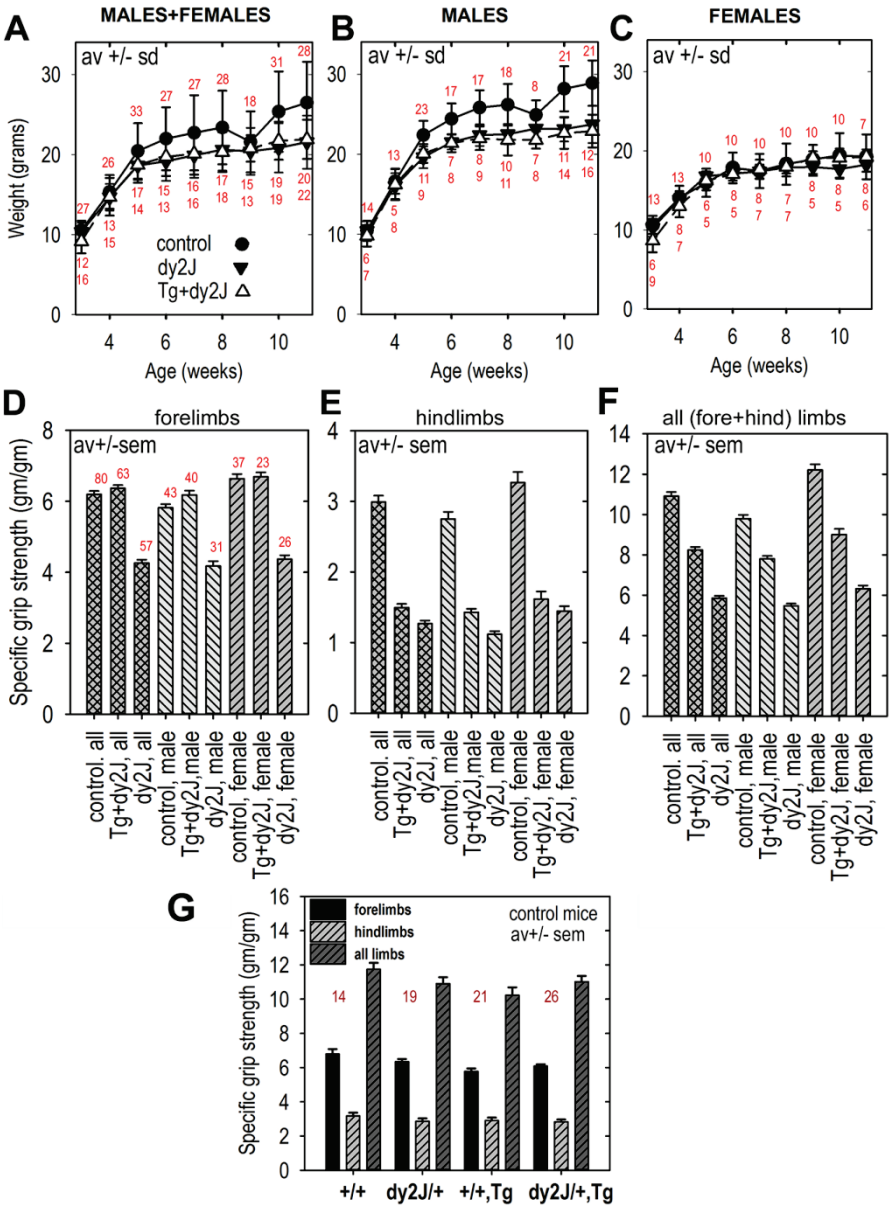

Supplemental Figure 1. *Stratification of adult weights and grip strength measurements*. **Panels A-C**. Male and female mice were weighed between 3 and 11 weeks of age (average +/- sd; number of mice indicated in red adjacent to bars). **Panels D-F**. Specific grip strengths were determined for mice 8-11 weeks of age and stratified by sex and limbs (average +/- sem, number of mice shown in red). **Panel G**. Normal mouse grip strengths (8-11 weeks) separated by genotype. Adult female mice weighed less than adult males. Female dystrophic mice were indistinguishable from control females but male dystrophic mice weigh less than control males. Reductions in specific grip strength were similar for males and females as were the improvements in grip strength due to αLNNd transgene (Tg) expression. No significant differences were noted among homozygous wild-type and heterozygous (dy^{2J}/+) mice with/without transgene.

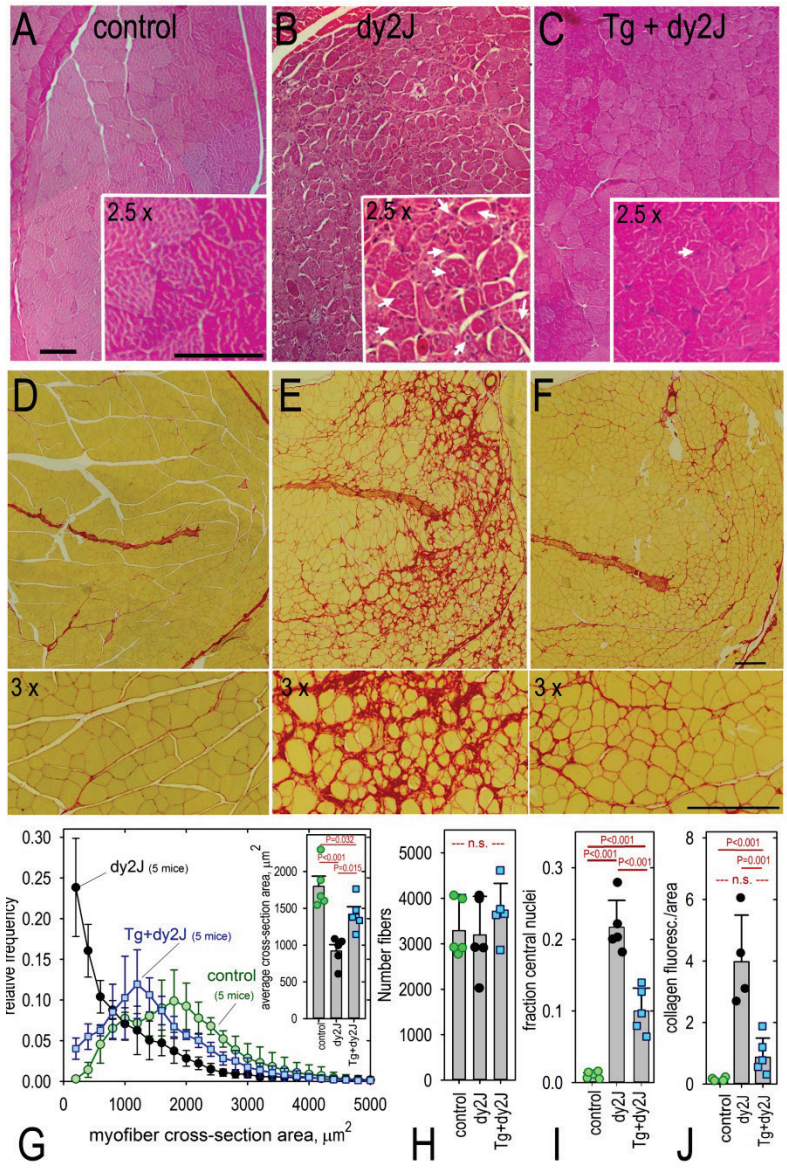

Supplemental Figure 2. *Hindlimb muscle histology.* **A-C**. Haematoxylin and eosin stains of paraffin sections of rectus femoris (11 weeks age). Size bars, 100 μm. White arrows indicate examples of central nuclei in 2.5x magnified insets. Homozygous *dy2J* myofibers have variable sizes, are often rounded, and have frequent central nuclei indicative of increased regeneration. Dystrophic muscle expressing the transgene have a morphology similar to that of control muscle. **D-F**. Picro-Sirius red collagen stain of adjacent sections. Size bar, 200 μm upper panels, 100 μm lower in 3x panels. A substantial increase in fibrosis (red stain) between myofibers and sometimes replacing myofibers is seen in the homozygous *dy2J* muscle. This is greatly reduced in *dy2J* muscle with transgene. **G**. Histogram of distribution of cross-sectional myofiber areas comparing control, *dy2J* and αLNNd Tg+*dy2J* mice (av+/-s.d., n=5 mice/condition). Inset: Overall average of myofiber cross-sectional areas (average +/- s.e.m., n=5 mice/condition). The smaller-size area distribution of *dy2J* is increased in the presence of transgene to one approaching that of control muscle. **H**. Total count of myofibers in rectus femoris cross-sections (av +/- s.d., n=5 mice/condition) was similar for the three conditions (unlike extensor carpi radialis). **I.** Fraction of myofibers with central nuclei (regeneration). **J**. Sirius red fluorescence determined by indirect fluorescence microscopy shows reduced fibrosis in *dy2J* muscle with transgene (av+/- s.d., n=4 controls, 4 dy2J, and 5 Tg+dy2J). Individual mouse values (colored and black circles) superimposed on bar averages.

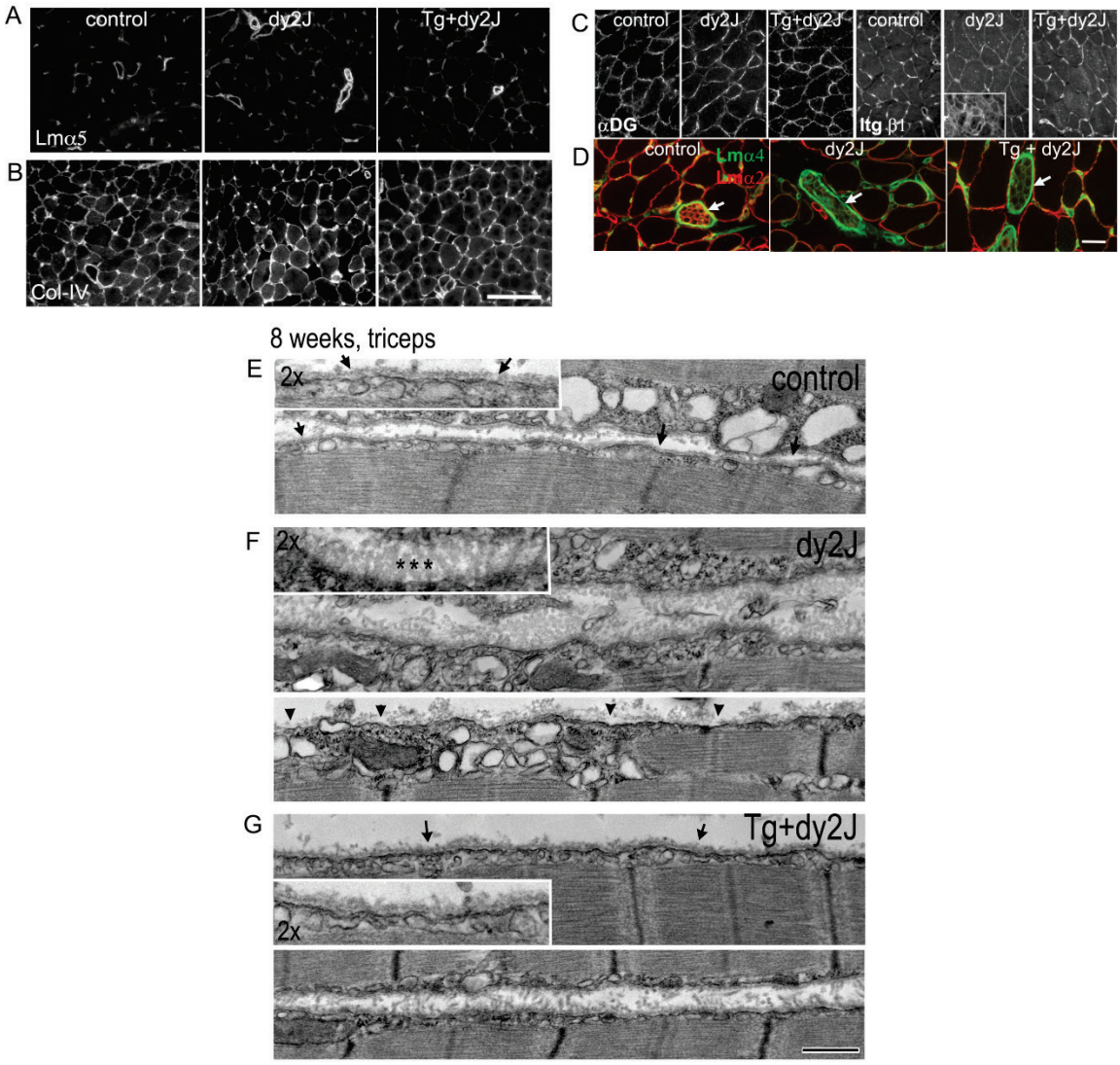

Supplemental Figure 3. *Muscle Lmα5, collagen type IV, integrin and dystroglycan immunofluorescence and electron microscopy.* **A-D**. Immunostained cryosections of triceps muscle (littermates, 4 weeks age). Staining with Lmα5 (A) and collagen-IV (B) antibodies. Lmα5 and collagen-IV immunostaining is similar in control, *dy2J*, and *dy2J* with transgene (Tg + *dy2J*) muscle. Size bar, 100 μm. Little Lmα5 outside of capillaries is detected. C. Sections stained with antibody to αDG and β1 integrins. No differences among control, *dy2J* and Tg + *dy2J* are appreciated in αDG stained sections. Integrin immunostaining is similar for the mice except in *dy2J* muscle in regions of active regeneration where it is noted to be increased (inset). D. Peripheral nerve (arrows) in Lmα4/Lmα2 co-stained muscle. Size bar, 25 μm. Endoneurial and perineurial BMs exhibit Lmα4 and Lmα2 staining. Lmα2 is reduced relative to Lmα4 in dystrophic muscle, regardless of the presence of muscle-specific transgene. **E-G**. *Myofiber ultrastructure.* Electron micrographs of triceps muscle (8 weeks age) from control (**+**/dy^{2J}, αLNNd, E), dy^{2J}/dy^{2J} ("*dy2J*", F), and αLNNd transgene-dy^{2J}/dy^{2J} littermates (G) (bar = 500 nm; BM indicated with arrows). The *dy2J* muscle appearance differs from that of both control and Tg + *dy2J*. The *dy2J* abnormality consists of irregular attenuations, rarifications and interruptions (arrowheads) of the sarcolemmal BM with intervening stretches that are denser and more continuous. Increased number and density of interstitial collagen fibrils adjacent to and often impinging on (inset, asterisks) the sarcolemmal plasma membrane are seen. The *dy2J*/transgene sarcolemmal BM (and adjacent collagen fibril pattern), on the other hand, is similar to that of controls. The BM ultrastructural abnormality in *dy2J* increases with age, which may also be concurrent with the deposition of fibrous collagens.

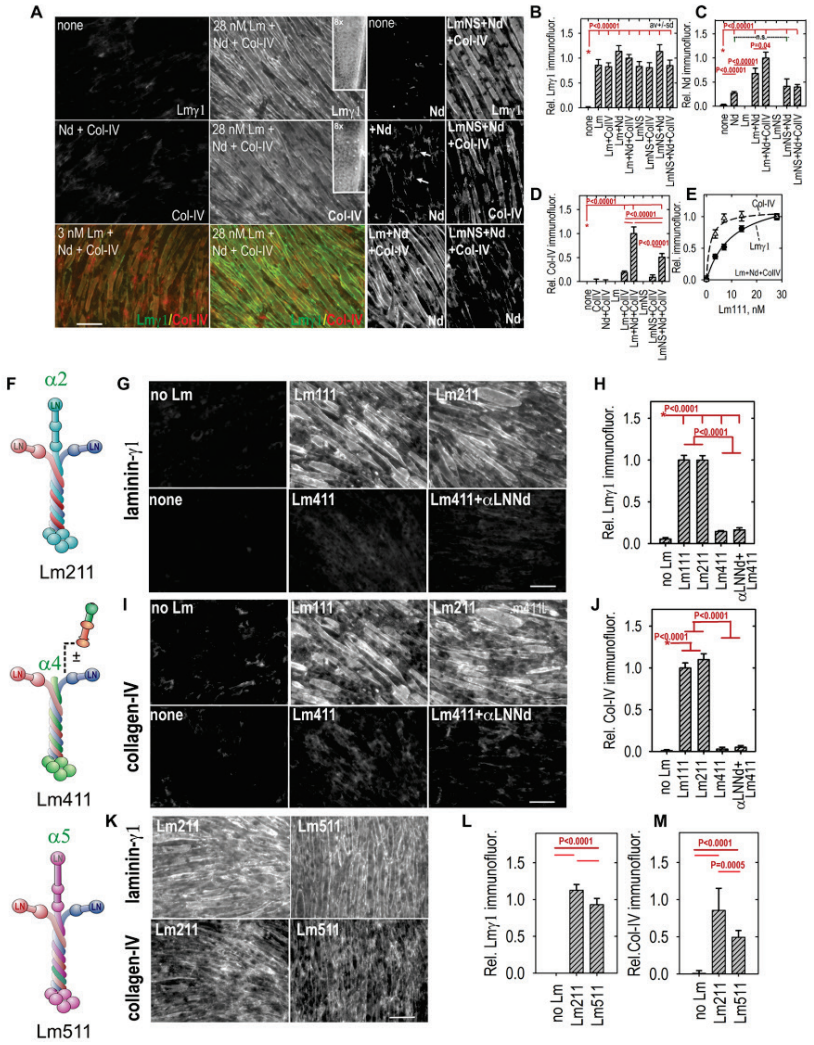

Supplemental Figure 4. *Contributions of laminins, nidogen and collagen-IV to BM assembly on C2C12 myotube lawns*. **A-E.** Purified laminin-111 (or Lm111-γ1*N802S* that cannot bind to nidogen), nidogen-1, and EHS matrix-derived type IV collagen were added to the culture medium of C2C12 myotubes for 1 hour at 37°C, washed, fixed, and immunostained with antibodies to the Lmγ1 subunit, nidogen-1, and type IV collagen. Bar, 200 μm. Panel A. Immunofluorescence images are shown for the indicated conditions (no protein treatment ("none"); 28 nM nidogen-1 (Nd) and 14 nM type IV collagen (Col-IV), 28 or 3 nM laminin-111 (Lm), and 28 nM Lm111-γ1*N802S* (LmNS). Insets show magnified (8x) segments of myotubes with a characteristic pre-costameric pattern. Panels B-D**.** Plots of summed immunofluorescence intensities for Lm111, nidogen-1 and collagen-IV determined from segmented images relative to maximal values (average +/- s.d., n= 7-10 10x-fields). **E.** Lmγ1 and type IV collagen immunofluorescence plotted as a function of Lm111 concentration (av. +/- s.d., 6-8 fields/condition, with data fitted for simple binding). Laminin accumulated on myotube surfaces in the absence of the other components. Type IV collagen accumulation reached a plateau at low Lm111 concentrations. *Assembly of laminin isoforms*. **F-M**. Laminin isoforms. Myotubes were treated as above with 28 nM Lm111, Lm211, and Lm411 (G-J), and rLm511 compared to Lm211 (K-M) in the presence of 28 nM nidogen-1 and 14 nM collagen-IV. Representative images and plots (av+/- s.d., n=7 to 10 10x fields/condition) of average laminin and collagen-IV immunostaining are shown in G, I and K. Size bars, 200 μm. Significance was assessed by one-way ANOVA with pairwise Holm-Sidak comparisons. While Lms 111, 211 and 511 were similar in their accumulation, almost no Lm411 accumulation was detected. This low level was only increased slightly when co-incubated with equimolar αLNNd.

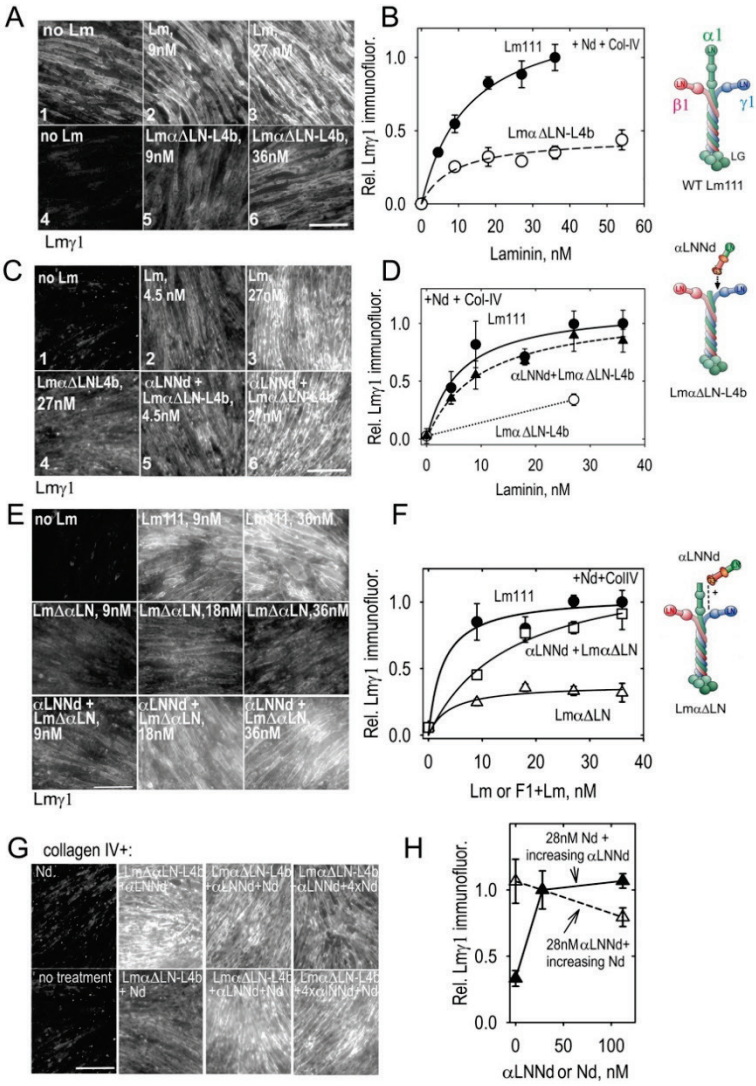

Supplemental Figure 5.*Concentration-dependency of αLNNd-laminin polymerization and effect of changing the αLNNd/nidogen ratio.* **A-F**. *αLNNd/laminin concentration dependency*: C2C12 myotube lawns were treated with increasing concentrations of wild-type Lm111, non-polymerizing LmαΔLn-L4b, and non-polymerizing LmαΔLN in the absence and presence of αLNNd equimolar to laminin in the presence of 28 nM nidogen-1 and 14 nM collagen-IV. Representative immunofluorescence images of myotubes stained with Lmγ1 antibody are shown in **A, C**, and **E** (10x objective, bar equal 200 μm). Corresponding plots of the average net Lmγ1 immunofluorescence are shown in **B, D** and **F** (average +/- s.d, n= 6 to 7 fields in B, 6 to 8 fields in D, and 8 to 10 fields in F). Polymerizing Lm111 (WT) accumulated on myotubes 2-3 higher compared to non-polymerizing laminins (Lmα1ΔLN-L4b and Lmα1ΔLN). αLNNd increased Lmα1ΔLN-L4b and Lmα1ΔLN to levels nearly equal to that of WT Lm111, with maximum accumulation occurring at lower αLNNd levels in Lmα1ΔLN-L4b compared to Lmα1ΔLN. **G,H**. *Competition between αLNNd and nidogen on C2C12 myotubes*. αLNNd binds to the same locus in Lmγ1 as nidogen-1, leading to the prediction that the two proteins compete for laminin-binding. C2C12 myotubes were treated with different ratios of αLNNd and nidogen-1 (Nd) co-incubated with 28 nM Lmα1ΔLn-L4b in the presence of 14 nM type IV collagen. Representative Lmγ1 immunofluorescence images shown in G (bar, 200 μm) and corresponding plot in H (av +/- s.d., n = 6 to 10 fields). Increasing the nidogen/αLNNd ratio with a non-polymerizing laminin decreased laminin accumulation on myotubes, whereas increasing the αLNNd/nidogen ratio increased laminin accumulation.